Spectrochimica Acta Part A: Molecular and Biomolecular Spectroscopy 211 (2019) 356–362

Contents lists available at ScienceDirect

Spectrochimica Acta Part A: Molecular and Biomolecular Spectroscopy

journal homepage: www.elsevier.com/locate/saa

Inspecting human colon adenocarcinoma cell lines by using terahertz time-domain reflection spectroscopy

Yuqi Cao [a], Jiani Chen [b], Pingjie Huang [a,*], Weiting Ge [b], Dibo Hou [a], Guangxin Zhang [a,*]

[a] State Key Laboratory of Industrial Control Technology, College of Control Science and Engineering, Zhejiang University, Hangzhou, People's Republic of China
[b] Cancer Institute, The Second Affiliated Hospital, Zhejiang University School of Medicine, Hangzhou, People's Republic of China

ARTICLE INFO

Article history:
Received 10 October 2018
Received in revised form 10 December 2018
Accepted 11 December 2018
Available online 11 December 2018

Keywords:
Terahertz time-domain attenuated total reflection spectroscopy
HT-29 cell line
DLD-1 cell line
Absorption coefficient
Dielectric loss tangent
Cancer identification

ABSTRACT

Techniques to inspect and analyze human colorectal cancer cell lines by using terahertz time-domain attenuated total reflection spectroscopy (THz TD-ATR) were investigated. The characteristics of THz absorption spectra of two colorectal cancer cell lines DLD-1 and HT-29 in aqueous solutions with different concentrations were studied. Different spectral features were observed compared to normal cell line. Identification results based on different parameters including absorption coefficient, refractive index, real and imaginary parts of complex permittivity, dielectric loss tangent were discussed. This research may be promising for quick and instant inspection of liquid samples by using THz time-domain spectroscopy in medical applications.

1. Introduction

Colon cancer is one of the best-understood tumors, but it remains one of the most common causes of cancer-related death. Some of its cancer cells are still not treated by existing therapies [1,2]. At present, the main clinical diagnosis technique for colon cancer is to perform a fecal occult blood test and colonoscopy. So far, the fecal occult blood test generally has a risky rate of missed diagnosis, especially for patients with a lower grade of colon cancer. Furthermore, the colonoscopy is expensive and painful [3]. It is noteworthy that, compared with the traditional pathological biopsy, the liquid biopsy is simpler and more non-invasive. It can achieve the purpose of sampling at any time and monitor in real time, especially in patients with deep-site tumors and clinically difficult to obtain satisfactory tissue samples. Owing to these advantages the relevant liquid biopsy-related technology platform has been continuously improved and stabilized, and liquid biopsy has received increasing attention.

For example, the human colon adenocarcinoma cell lines HT-29 and DLD-1 have been used to study the biology of human colon cancers. The replacement of glucose by galactose in the culture medium induced a reversible enterocytic differentiation, HT29 cells have become a unique model for studying the molecular mechanisms of intestinal cell differentiation [4,5]. The study of these two human colon adenocarcinoma cell lines is very useful for understanding human colon cancer transformation. It has been proved that, there can be only one colon cancer cell line in each colon cancer patient [6]. Because the diversity of cancer cell lines that cause colon cancer, the simultaneous identification of these two cancer cell lines from normal cell line will increase the possibility of recognizing colon cancer.

Terahertz wave is an emerging non-destructive testing technology with frequency band from about 0.1 to 10 THz. Since terahertz wave is low-energy and non-ionizing, it does not only cause any harm to biological macromolecules, cells, and tissues, but provide a direct measurement of the field amplitude and phase, which are related to the absorption coefficient and the permittivity of the sample [7–9]. Furthermore, terahertz wave is sensitive to polar molecules, especially to biomacromolecules as the energy level of terahertz radiation is close to the low-frequency motion of biomolecules such as the vibration, rotation and translation of the molecular skeleton. For these reasons, terahertz technology has been investigated to identify biomolecules with fingerprint features. THz spectroscopy method is potential for applications in medical diagnostics owing to its unique detection properties [10–14].

In addition, terahertz time-domain attenuated total reflection spectroscopy has become an important inspection method for aqueous solution of various tumor markers and other cancer related substances [15–21]. For instance, the global hydration state of saccharides was investigated by THz TDS-ATR spectroscopy. The complex refractive

* Corresponding authors.
E-mail addresses: huangpingjie@zju.edu.cn (P. Huang), gxzhang@zju.edu.cn (G. Zhang).

https://doi.org/10.1016/j.saa.2018.12.023
1386-1425/

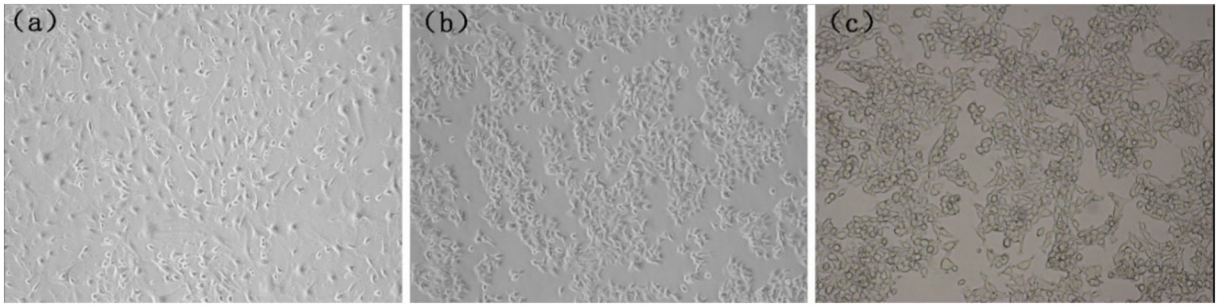

Fig. 1. Morphology of three cell lines after magnification by 100× under the microscope. (a) 3 T3 cells; (b) DLD-1 cells; (C) HT-29 cells.

index of saccharide was used to analyze the characteristics of the global hydration state. Their results suggested that the global hydration state was closely related to the number of hydrophilic groups and steric configuration of hydroxyl groups in saccharide molecules [15]. Furthermore, the hydration state inside HeLa cell monolayer was studied using THz TDS-ATR spectroscopy since the hydration state in living cells had not been investigated to date. The authors found that 23.8 ± 7.4% of the HeLa intracellular water was bound to biomolecules such as proteins, RNA, and DNA. The intracellular hydration water molecules showed slower reorientation dynamics relative to that of bulk water [16]. The vibrational spectra of solid-state DNA nucleobases were studied and the vibrational modes corresponding to the main peaks in the experimental spectra were assigned with the PBC-GEBF results. The calculation results were in good agreement with the experimental data. The results of the harmonic vibrational frequency indicated that all the vibrational modes belong to collective vibrational modes, which involve complicated mixtures of intermolecular and intramolecular displacements about 0.5 to 9 THz [17]. Though some research about recognizing cancer related substances has been carried out, there is little research on colon cancer cell lines.

Based on this background, we have attempted to apply THz TD-ATR spectroscopy to do the cancer cell lines identification which can provide a preliminary experimental basis for liquid biopsy. In this study, the differences in terahertz absorption characteristics between two colorectal cancer cell lines DLD-1 and HT-29 samples were investigated by employing THz TD-ATR spectroscopy. The dependence of the absorption coefficient of cancer cells on different concentrations was also studied. In addition, we proposed an identification method to classify samples into normal and cancerous groups. The satisfactory classification result suggests that methodology could be applied to automatic discrimination of human colon cancer cell lines and then to identify cancer situations with terahertz techniques.

2. Experiment

2.1. Experimental Setup

The commercial THz TD-ATR system applied in this paper were developed by Advantest Corporation in Japan. A silicon ATR prism of a THz TD-ATR spectrometer, TAS7500 was employed. The optical excitation in this system is achieved by an optical fiber femtosecond laser that produces fewer than 50 fs pulses at center wavelength around 1550 nm, with a repetition rate of 50 MHz and an average power of 20 mW. The experiments were carried out at room temperature (300 K) and the humidity was kept at about 2%. The system gives an available frequency range of 0.1 to 3.0 THz, but when the sample is in an aqueous phase, the valid range tends to decrease due to signal attenuation by the sample.

2.2. Sample Preparation

In this experiment we used human colon cancer epithelial cell lines (HT-29, DLD-1) and mouse fibroblast epithelial cells (NIH/3 T3). These cell lines were all purchased from Cell Bank of Shanghai Institutes for Biological Sciences of Chinese Academy of Sciences. The mouse fibroblast epithelial cells were used as normal cell line because mouse fibroblasts are similar to human fibroblasts in structure and are readily available. All cells were cultured in an incubator in which the temperature was kept at 37 °C with 5% CO_2 using RPMI-1640 medium. After the cells had grown to logarithmic phase, they were collected into a blood cell count plate and counted under a microscope for three times. The average value was taken as the cell number. According to the counting results, the final cell suspension concentration was adjusted to 5×10^6 cells/ml. The cell suspension with a certain concentration gradient was obtained by multiple dilutions, and the concentrations were 5×10^6

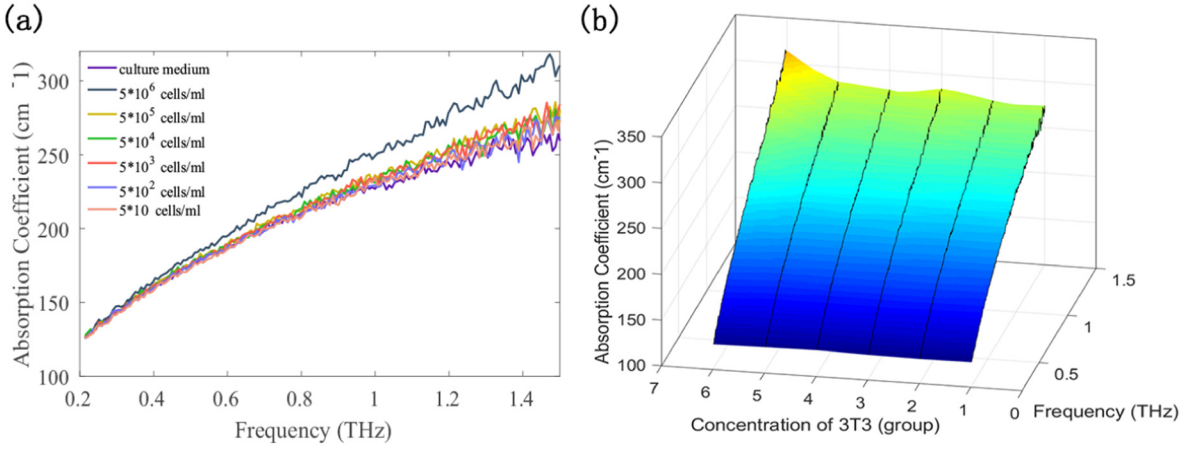

Fig. 2. (a) Absorption coefficients of 3 T3 cell solutions at concentrations from 50 cells/ml to 5×10^6 cells/ml. (b) Concentration dependence of the absorption coefficient for 3 T3 cell solutions from 0.2 to 1.5 THz.

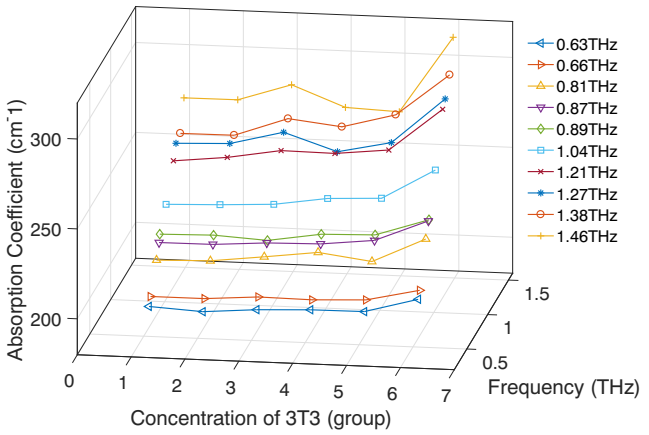

Fig. 3. Dependence of the absorption coefficient of 3 T3 cells on different concentrations between 0.6 and 1.5 THz.

cells/ml, 5×10^5 cells/ml, 5×10^4 cells/ml, 5×10^3 cells/ml, 5×10^2 cells/ml, 5×10 cells/ml, respectively. The results of the three cell lines cultured in RPMI-1640 medium at a magnification of 100× under the microscope are shown in Fig. 1.

In this study, since the cells are heavier than the medium, they will go down to the bottom. Therefore, every time before we dropped the sample, we used a blank pipette tip to blow the cell solution evenly. In addition, we obtained 8 valid sample drops for each concentration of the three cell lines. The content of each drop was 400 μl. In total, the spectra from 48 normal cell sample drops and 96 cancerous cell sample drops which included two cancer cell lines were studied. For the referenced group, we also tested 8 drops of RPMI-1640 medium with the same content of sample drops. In order to make sure the system was stable, we tested the spectrum of distilled water after every 4 drops.

2.3. Data Analysis

Complex refractive index is often used to indicate the optical properties of a substance [22,23].

$$\tilde{n}(\omega) = n(\omega) - \mathrm{j}\kappa(\omega) \tag{1}$$

In Eq. (1), $n(\omega)$ and $\kappa(\omega)$ are the refractive index and the extinction coefficient, respectively. Moreover, the absorption coefficient is calculated using and shown in Eq. (2) [24].

$$\alpha(\omega) = \frac{2\omega\kappa(\omega)}{c} \times 10^{10} \tag{2}$$

In addition, biological macromolecules are typical dielectric materials with dipole characteristics. Changes in polarization properties caused by changes in the structure of biomolecules can be reflected in the complex permittivity of the terahertz field.

$$\varepsilon(\omega) = \varepsilon_1(\omega) - i\varepsilon_2(\omega) \tag{3}$$

where $\varepsilon(\omega)$ is the complex relative dielectric constant in Eq. (3). $\varepsilon_1(\omega)$ and $\varepsilon_2(\omega)$ show the real and imaginary parts of the complex dielectric constant, respectively.

$$\tan\delta = \frac{\varepsilon_2(\omega)}{\varepsilon_1(\omega)} \tag{4}$$

The dielectric loss tangent, shown in Eq. (4), is defined as the ratio of the imaginary part of the complex permittivity to the real part [25,26]. This parameter reflects the energy consumed by the material during the conversion of electromagnetic energy into heat energy and it is sensitive to the dynamic changes of the protein side chains.

The valid frequency of the spectra analyzed ranged from 0.2 to 1.5 THz, which escaped from the strong noise associated with higher frequencies. The spectra presented in Sections 3.1 and 3.2 are the average spectra of all 8 sample drops with the same concentration while we applied all the data in the classification.

3. Results and Discussion

3.1. THz Spectral Characteristic of Normal Cell Line

The absorption coefficients of 3 T3 cell solutions at concentrations from 50 cells/ml to 5×10^6 cells/ml and the concentration dependence of the absorption coefficient for 3 T3 cell solutions from 0.2 to 1.5 are respectively shown in Fig. 2. The 1 to 6 groups for concentration represent 5×10 cells/ml, 5×10^2 cells/ml, 5×10^3 cells/ml, 5×10^4 cells/ml, 5×10^5 cells/ml, 5×10^6 cells/ml, respectively. The 3 T3 cell solutions did not show any significant distinct peaks in the absorption spectra. In addition, Fig. 2 shows a positive correlation between frequency and absorption coefficient for each concentration. However, it also shows that the amplitude changes in absorption spectra of 3 T3 cell solutions with different concentrations are highly nonlinear. The absorption coefficients do not simply decrease at the same frequency with lower concentrations. Although the absorption of the 5×10^6 cells/ml solution

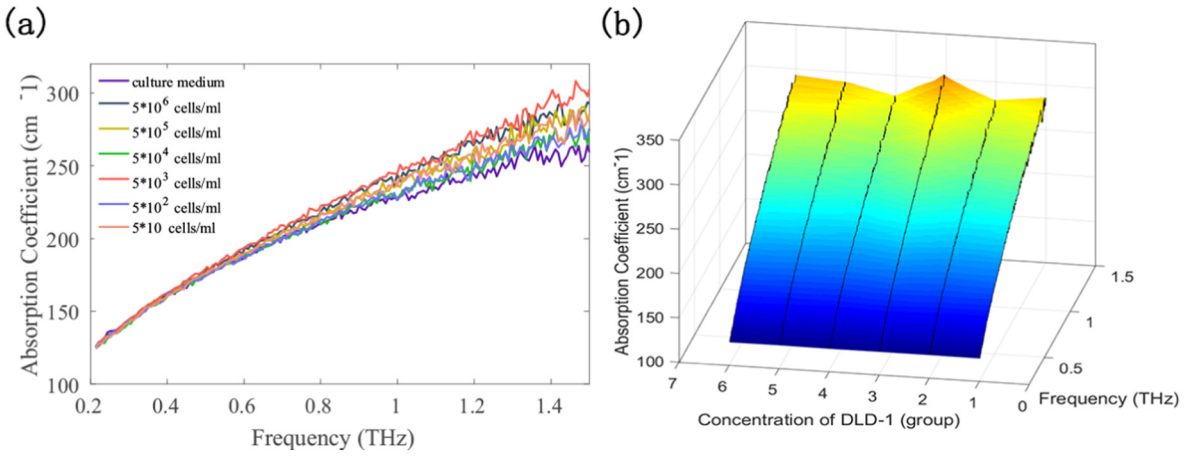

Fig. 4. (a) Absorption coefficients of DLD-1 cell solutions at concentrations from 50 cells/ml to 5×10^6 cells/ml. (b) Concentration dependence of the absorption coefficient for DLD-1 cell solutions from 0.2 to 1.5 THz.

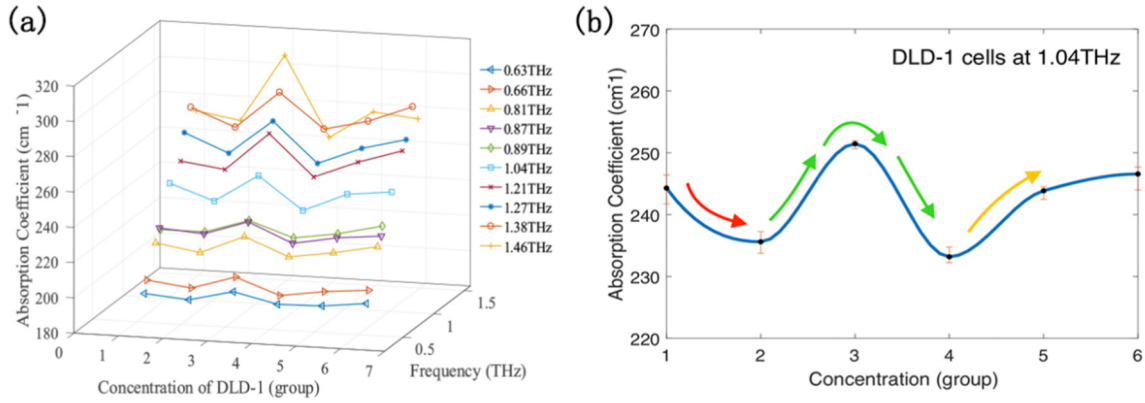

Fig. 5. (a) Dependence of the absorption coefficient of DLD-1 cells on different concentrations between 0.6 and 1.5 THz. (b) The absorption coefficient of DLD-1 cells at 1.04 THz as a function of concentration.

appears strongest, the absorption coefficients for other concentrations do not appear to be in order. We give the absorption coefficients against concentration for 3 T3 cells from 0.63 to 1.46 THz in Fig. 3. The relationship between the absorption coefficient and both frequency and concentration are shown in order to highlight the characteristics.

The method for obtaining these frequency points in Fig. 3 is to find the frequency points of co-existing peaks in the frequency range from 0.2 to 1.5 in the absorption coefficient spectra of 6 different concentrations of cells. Only a part of the characteristic frequency points is taken, in order to facilitate the observation of the result. Thus, the terahertz absorption at different cell concentrations is analyzed at these characteristic frequency points. It can also be seen from Fig. 3 that for 3 T3 cells, except at 0.81 THz, 1.27 THz, 1.38 THz and 1.46 THz, the absorption does not exhibit a linear increase with increasing concentration. The slight fluctuation at 0.81 THz was caused by water absorption since water has absorption peaks around 0.75, 1.35, and 1.46 THz in room temperature [27]. In addition, when the frequency is higher than 1.3 THz, the strong attenuation of terahertz waves could cause the absorption coefficient to fluctuate slightly. Therefore, apart from these influence, the absorption coefficient of normal cell line in mice almost continuously increases with increasing concentrations.

3.2. THz Spectral Characteristics of Human Colon Adenocarcinoma Cell Lines DLD-1 and HT-29

Fig. 4 shows the absorption coefficients of DLD-1 cell solutions at six concentrations from 50 cells/ml to 5×10^6 cells/ml as well as concentration dependence of the absorption coefficient for DLD-1 cell solutions from 0.2 to 1.5 THz. As with 3 T3 cells, there are not any clear distinctive peaks.

From Fig. 5, the DLD-1 cell solutions do not follow the Beer–Lambert law, since the relationship between the absorption coefficient and concentration is clearly nonlinear. In addition, we can see that the absorption coefficient slightly reduces with increasing DLD-1 cells concentration until 5×10^2 cells/ml in Fig. 5. After that, the absorption coefficient keeps increasing, reaching its maximum at 5×10^3 cells/ml. Then, the absorption coefficient rapidly decreases until 5×10^4 cells/ml. When the concentration increases further, the absorption coefficient increases again. Furthermore, we also find the absorption coefficient has a smaller fluctuation at low frequency and it fluctuates more intense at high frequency. The trend of absorption coefficient with increasing concentration can be related to the interactions and hydration state of the cells exist at different concentrations.

This is related to the "terahertz excess" and "terahertz defect" caused by the hydration state of the cells [28–30]. In order to further observe the effect of the concentration on the terahertz absorption characteristics of the DLD-1 cells, Fig. 5(b) shows the absorption coefficient of DLD-1 cells at 1.04 THz as a function of concentration. At the lower concentrations from 50 to 500 cells/ml, DLD-1 cells are not surrounded by dynamical hydration shells. At these two concentrations, the solution consists of two parts: solute and bulk water, and the absorption of bulk water dominate. The absorption coefficient of bulk water in the terahertz region dominates, therefore, with the increase of concentration, the absorption coefficient decreases since water was pushed out of the way by cells (see red arrow of Fig. 5(b)). However, the hydration shell begins to form at approximately 5×10^2 cells/ml which cause the

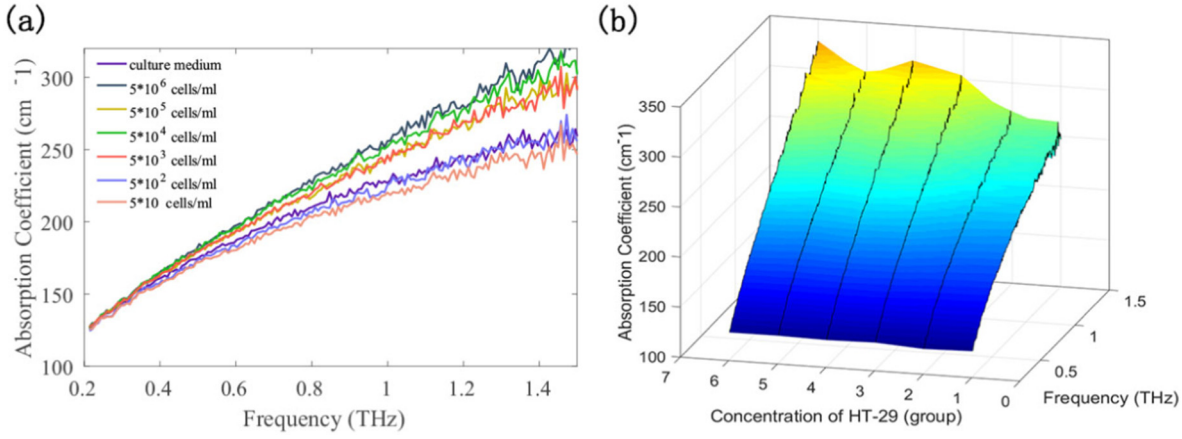

Fig. 6. (a) Absorption coefficients of HT-29 cell solutions at concentrations from 50 cells/ml to 5×10^6 cells/ml. (b) Concentration dependence of the absorption coefficient for HT-29 cell solutions from 0.2 to 1.5 THz.

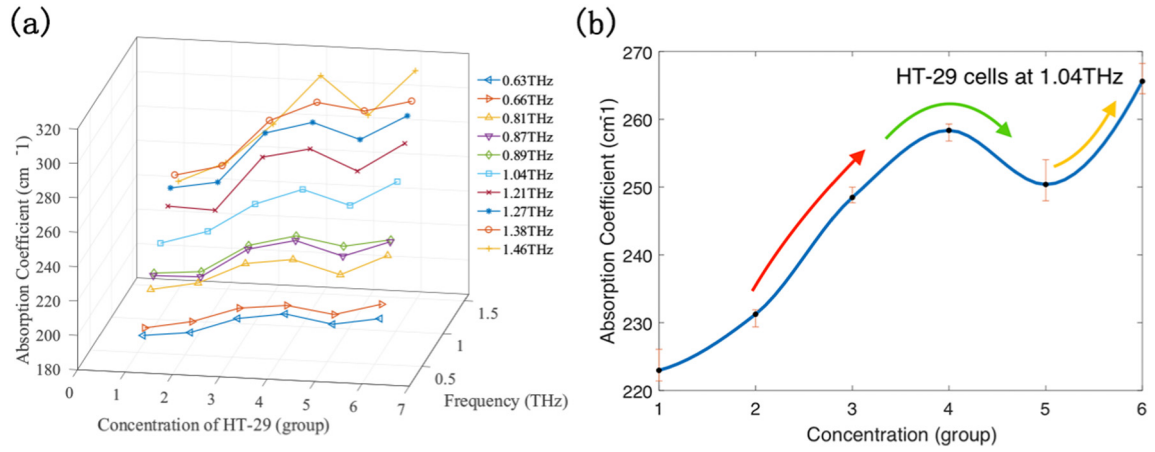

Fig. 7. (a) Dependence of the absorption coefficient of HT-29 cells on different concentrations between 0.6 and 1.5 THz. (b) The absorption coefficient of HT-29 cells at 1.04 THz as a function of concentration.

absorption coefficient to start increasing. In solutions, the absorption of the hydration shell is greater than that of the bulk water which leads to the increase of absorption coefficient as the concentration is further increased (see green arrow of Fig. 5(b)). Then, the hydration shells become saturated at about 5×10^3 cells/ml that resulted in a decrease in the absorption coefficient again until 5×10^4 cells/ml. However, as the concentration continues to increase, the absorption of the cells themselves becomes stronger which results in an increase in the absorption coefficient.

As for HT-29 cells, we can see several different characteristics. The absorption coefficients of HT-29 cells at the six concentrations and the concentration dependence of the absorption coefficient for HT-29 cells from 0.2 to 1.5 are shown in Fig. 6, respectively. And the dependence of the absorption coefficient of HT-29 cells on different concentrations between 0.6 and 1.5 THz are shown in Fig. 7(a).

From Fig. 7(a), we also see that the HT-29 cell solutions do not follow the Beer–Lambert law, though there is an overall upward trend. The absorption coefficient stably increases with increasing HT-29 cells concentration up to 5×10^4 cells/ml. Then, the absorption coefficient decreases until 5×10^5 cells/ml. After that, the absorption coefficient continuously increases to 5×10^6 cells/ml.

Fig. 7(b) indicates that there are hydration shells surrounding the cells since the lowest concentration and the number of hydration shells keeps increasing as the concentration goes up. It can also be seen that the absorption of the hydration shell in the terahertz region is higher than that of the bulk water as well as HT-29 cells. Therefore, the absorption coefficient shows an increasing trend as the concentration increases (see red arrow of Fig. 7(b)). After that, the hydration shells begin to saturate until about 5×10^4 cells/ml, leading to a decrease in the absorption coefficient. However, as the concentration continues to increase, the absorption of the cells themselves becomes stronger which results in an increase in the absorption coefficient from the concentration of 5×10^5 cells/ml. As shown in Figs. 5(b) and 7(b), there are different features in the absorption spectra by two human colon adenocarcinoma cell lines from different patients of different concentrations. In addition, the characteristics in the absorption spectra of the two cell lines are significantly different from the normal cells. Therefore, the use of THz TD-ATR technique to detect liquid cancer cell lines has certain rationality.

3.3. Cancer Cell Lines Recognition Method

In order to explore the classification and discrimination effects on cancer cell lines and to find the most suitable spectral parameters, this study combines the machine learning method k-nearest neighbors (KNN) which is suitable for small-sample classification to try to differentiate two cell line groups. In the process of classification, we identified two types of cancer cell lines as cancer cell samples at the same time. In fact, every colon cancer patient will only have a single colon cancer cell line. Therefore, if multiple cancer cell lines can be detected at the same time, colon cancer patients with different cancer cell lines can be diagnosed. This can enhance the generalization ability of the model. The flow chart of the cancer cells discrimination algorithm based on sensitive parameters of terahertz spectra is shown in Fig. 8.

Since the number of normal cell samples is smaller than that of cancer cells in the experiment, the KNN method is applied to classify and recognize the unbalanced number of samples [31]. KNN is a case-based learning method, which keeps all the training data for classification. One way to improve its efficiency is to find some representatives to represent the whole training data for classification, viz. building an

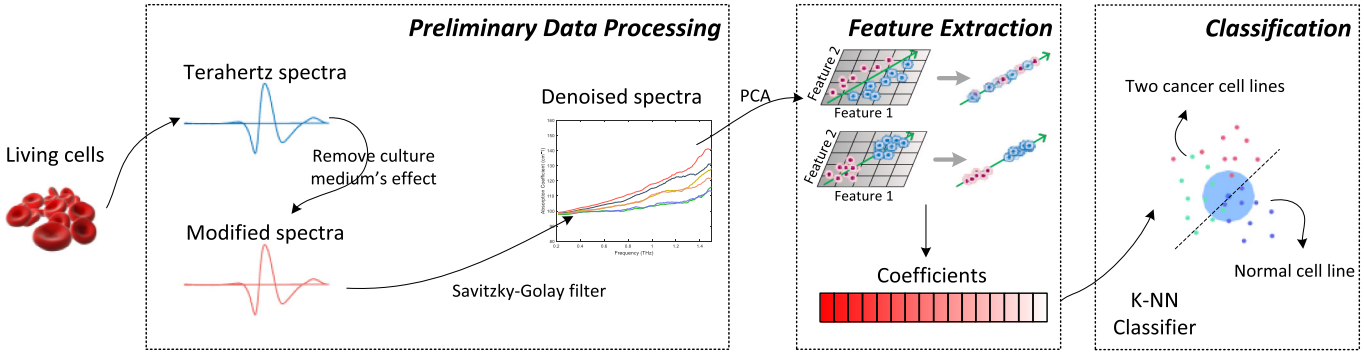

Fig. 8. Flow chart of cancer cell lines discrimination algorithm based on sensitive parameters of terahertz spectra.

Table 1
Prediction of results based on models of different parameters.

Parameter	Accuracy	Sensitivity	Specificity
Absorption coefficient	88.9%	93.9%	75.0%
Refractive index	84.4%	91.0%	66.7%
Real part of complex permittivity	82.2%	87.9%	66.7%
Imaginary part of complex permittivity	84.4%	87.9%	75.0%
Dielectric loss tangent	86.7%	91.0%	75.0%

inductive learning model from the training dataset and using this model for classification [32]. Firstly, the terahertz spectra of the corresponding parameters are subjected to an operation of removing the disturbance of the culture medium. Specifically, the terahertz spectra of different cell concentrations subtract the corresponding parameter spectra of the culture medium, and then increase the specified coefficient so as to ensure that the amplitude is positive. Then, the S-G algorithm is performed to denoise the spectra. After that, principal component analysis is used to extract features of the data, and the first three principal components are taken as data features. Finally, the principal component feature vector is taken as the input of KNN.

3.4. Identifying Human Colon Adenocarcinoma Cell Lines From the Normal Cell Line

The results obtained by using different parameters and performing a five-fold cross-validation of the data are shown in Table 1, in which not only the optical coefficients like absorption coefficient and refractive index are used, but also the dielectric parameters such as complex permittivity and dielectric loss tangents. The preprocessed terahertz spectra with different parameters are applied as input to the classifier. As shown in the results, there are obvious differences in the modeling effects of different parameters. The real part of the complex permittivity shows the worst results while the imaginary part of complex permittivity and refractive index has slightly better recognition results. Moreover, the recognition accuracy of the absorption coefficient and the dielectric loss tangent was significantly better than other parameters, with an accuracy of 88.9% and 87.4%, respectively.

The absorption coefficient and the dielectric loss tangent have a better discrimination sensitivity for normal cells and cancer cells. The dielectric loss tangent quantifies a dielectric material's inherent dissipation of electromagnetic energy to charge motion. Moreover, tan δ measurements are extremely sensitive to protein molecular relaxation and local motions in cells involving the reorientation of side-chains of residues as it is subjected to an oscillating electric field. The physical meaning of dielectric loss tangent can be related to the structure of cells and shows a good recognition effect. It is a dielectric parameter which has physical meanings to discriminate cancer cells. In addition, the absorption coefficient reflects the absorption characteristics of liquid cells. The difference in the spectra of this parameter between normal cell line and human colon adenocarcinoma cell lines may be due to changes in the intracellular protein structure.

4. Conclusion

In this paper, we applied terahertz spectroscopy to characterize two kinds of colorectal cancer cell lines. Based on the non-linear change of the absorption coefficient of cancer cell samples with six different concentrations, the detection ability of the terahertz spectroscopy technique on the hydration states of two different cancer cell lines was studied. The study found that the DLD-1 and HT-29 cell lines have appeared different hydration states since different cell compositions, which indicates the THz TD-ATR technique has the potential to detect liquid cancer cell lines. Subsequently, principal component analysis was used to extract coefficients of the 5 parameters for the recognition of cancer cells, and a discrimination model based on sensitive parameters was proposed. The results show that absorption coefficient and dielectric loss tangent have better detection capabilities for the identification of cancer cells. The results of this work are able to provide a preliminary experimental basis for liquid biopsy. This is a promising study for further research into the potential to use THz spectroscopy for high-sensitivity cancer cell lines testing and liquid biopsy applications in the future. Our next step would be exploring the mechanism of the spectral features of the two cancer cell lines, training with more samples to improve the accuracy and feasibility of the recognition model, and putting forward a more systematic identification solution.

Acknowledgements

This work was supported by the National Natural Science Foundation of China (No. 61873234, No. 61473255). We express our sincere thanks to Cancer Institute of the Second Affiliated Hospital for sample preparation.

References

[1] C.A. O'Brien, A. Pollett, S. Gallinger, et al., A human colon cancer cell capable of initiating tumour growth in immunodeficient mice[J], Nature 445 (7123) (2007) 106–110.
[2] S. Meeker, A. Seamons, J. Paik, et al., Increased dietary vitamin D suppresses MAPK signaling, colitis, and colon cancer[J], Cancer Res. 74 (16) (2016) 4398.
[3] E. Merika, M.W. Saif, A. Katz, et al., Review. Colon cancer vaccines: an update[J], In Vivo 24 (5) (2016) 607.
[4] D. Martínez-Maqueda, B. Miralles, I. Recio, HT29 Cell Line[M]//The Impact of Food Bioactives on Health, Springer International Publishing, 2015 113–124.
[5] M. Pinto, M.D. Appay, P. Simon-Assman, G. Chevalier, N. Dracopoli, J. Fogh, A. Zweibaum, Enterocytic differentiation of cultured human colon cancer cells by replacement of glucose by galactose in the medium[J], Biol. Cell. 44 (2) (1982) 193–196.
[6] A. Leibovitz, J.C. Stinson, C.E. Mccoy, et al., Classification of human colorectal adenocarcinoma cell lines[J], Cancer Res. 36 (12) (1976) 4562–4569.
[7] N. Bajwa, S. Sung, D.B. Ennis, et al., Terahertz imaging of cutaneous edema: correlation with magnetic resonance imaging in burn wounds[J], IEEE Trans. Biomed. Eng. PP (99) (2017) 1-1.
[8] Y. Cao, P. Huang, X. Li, et al., Terahertz spectral unmixing based method for identifying gastric cancer[J], Phys. Med. Biol. 63 (2018), 035016. (10pp).
[9] D. Hou, X. Li, J. Cai, et al., Terahertz spectroscopic investigation of human gastric normal and tumor tissues[J], Phys. Med. Biol. 59 (18) (2014) 5423–5440.
[10] M. Li, T. Chang, D. Wei, et al., Label-free detection of anti-estrogen receptor alpha and its binding with estrogen receptor peptide alpha by terahertz spectroscopy[J], RSC Adv. 7 (39) (2017) 24338–24344.
[11] D.Y. Chau, A.R. Dennis, H. Lin, et al., Determination of water content in dehydrated mammalian cells using terahertz pulsed imaging: a feasibility study[J], Curr. Pharm. Biotechnol. 17 (2) (2016).
[12] S. Yan, C. Yao, Challenge of the detection of circulating tumor cells with terahertz spectroscopy technique[J], Chin. J. Med. Phys. 33 (2018) 1225–1228.
[13] H. Chen, S. Ma, X. Wu, et al., Diagnose human colonic tissues by terahertz near-field imaging[J], J. Biomed. Opt. 20 (3) (2015) 36017.
[14] H. Cheon, H. Yang, S.H. Lee, et al., Terahertz molecular resonance of cancer DNA[J], Sci. Rep. 6 (2016) 37103.
[15] K. Shiraga, Y. Ogawa, N. Kondo, et al., Evaluation of the hydration state of saccharides using terahertz time-domain attenuated total reflection spectroscopy[J], Food Chem. 140 (1–2) (2013) 315–320.
[16] K. Shiraga, T. Suzuki, N. Kondo, et al., Hydration state inside HeLa cell monolayer investigated with terahertz spectroscopy[J], Appl. Phys. Lett. 106 (25) (2015) 861.
[17] F. Wang, D. Zhao, H. Dong, et al., Terahertz spectra of DNA nucleobase crystals: a joint experimental and computational study[J], Spectrochim. Acta A Mol. Biomol. Spectrosc. 179 (2017) 255–260.
[18] J. Shikata, H. Handa, A. Nawahara, et al., Terahertz ATR spectroscopy of liquids using THz-wave parametric sources[C]//lasers and electro-optics - Pacific Rim, 2007. CLEO/Pacific Rim 2007, Conference on. IEEE 2007, pp. 1–2.
[19] L. Chen, Y. Wei, X. Zang, Y. Zhu, S. Zhuang, Excitationof dark multipolar plasmonic resonances at terahertz frequencies[J], Sci. Rep. 6 (2016) 22027.
[20] X. Xu, Y. Wu, T. He, et al., Metamaterials-based terahertz sensor for quick diagnosis of early lung cancer[J], Chin. Opt. Lett. 15 (11) (2017) 84–86.
[21] L. Chen, N. Xu, L. Singh, et al., Defect-induced Fano resonances in corrugated plasmonic metamaterials[J], Adv. Opt. Mater. 5 (8) (2017) 1600960.
[22] L. Duvillaret, F. Garet, J.L. Coutaz, A reliable method for extraction of material parameters in terahertz time-domain spectroscopy[J], IEEE J. Sel. Top. Quantum Electron. 2 (1996) 739–746.
[23] T.D. Dorney, R.G. Baraniuk, D.M. Mittleman, Material parameter estimation with terahertz time-domain spectroscopy[J], J. Opt. Soc. Am. A Opt. Image Sci. Vis. 18 (7) (2001) 1562–1571.
[24] S.W. Smye, J.M. Chamberlain, A.J. Fitzgerald, et al., The interaction between terahertz radiation and biological tissue[J], Phys. Med. Biol. 46 (9) (2001) R101.

[25] Y. Sun, Z. Zhu, S. Chen, et al., Observing the temperature dependent transition of the GP2 peptide using terahertz spectroscopy[J], PLoS One 7 (11) (2012), e50306. .
[26] Y. Sun, J. Zhong, C. Zhang, et al., Label-free detection and characterization of the binding of hemagglutinin protein and broadly neutralizing monoclonal antibodies using terahertz spectroscopy[J], J. Biomed. Opt. 20 (3) (2015), 037006. .
[27] W. Withayachumnankul, B.M. Fischer, D. Abbott, Numerical removal of water vapour effects from terahertz time-domain spectroscopy measurements[J], Proc. Math. Phys. Eng. Sci. 464 (2097) (2008) 2435–2456.
[28] B. Born, M. Havenith, Terahertz dance of proteins and sugars with water[J], J. Infrared Millimeter Terahertz Waves 30 (12) (2009) 1245–1254.
[29] K. Meister, S. Ebbinghaus, Y. Xu, et al., Long-range protein-water dynamics in hyperactive insect antifreeze proteins[J], Proc. Natl. Acad. Sci. U. S. A. 110 (5) (2013) 1617.
[30] M. Heyden, M. Havenith, Combining THz spectroscopy and MD simulations to study protein-hydration coupling.[J], Methods 52 (1) (2010) 74.
[31] J. Zhang, I. Mani, kNN Approach to Unbalanced Data Distributions: A Case Study Involving Information Extraction[C]//in Proceedings of the ICML 2003 Workshop on Learning From Imbalanced Datasets, 2003.
[32] G. Guo, H. Wang, D. Bell, et al., KNN model-based approach in classification[J], Lect. Notes Comput. Sci 2888 (2003) 986–996.